International Journal of Nanoelectronics and Materials
Volume 14 (Special Issue) August 2021 [289-310]

Mathematical Modelling of Passive Discrete Lumped Parameter System using Standard Malaysian Rubber Constant Viscosity

Mohd Azli Salim[1,2,3*], Adzni Md. Saad[1,3], Feng Dai[4], Norbazlan Mohd Yusof[5], Nor Azmmi Masripan[1,2,3] and Aminurrashid Noordin[4]

[1]Fakulti Kejuruteraan Mekanikal, Universiti Teknikal Malaysia Melaka, Hang Tuah Jaya, 76100 Durian Tunggal, Melaka, Malaysia
[2]Advanced Manufacturing Centre, Universiti Teknikal Malaysia Melaka, Hang Tuah Jaya, 76100 Durian Tungggal, Melaka, Malaysia
[3]Intelligent Engineering Technology Services Sdn. Bhd., No.1, Jalan TU43, Taman Tasik Utama, 76450 Ayer Keroh, Melaka, Malaysia
[4]Institute of Science and Technology, China Railway Eryuan Engineering Group Co.Ltd, No.3 Tongjin Road, Sichuan, 610031, P.R. China
[5]Centre of Excellence, Projek Lebuhraya Usahasama Berhad, Menara Korporat, Persada PLUS, Persimpangan Bertingkat Subang, KM 15, Lebuhraya Baru Lembah Klang, 47301 Petaling Jaya, Selangor Darul Ehsan, Malaysia
[6]Fakulti Teknologi Kejuruteraan Elektrik dan Elektronik, Universiti Teknikal Malaysia Melaka, Hang Tuah Jaya, 76100 Durian Tunggal, Melaka, Malaysia

ABSTRACT

This paper represents the basic and circular vibration isolator in High Frequencies using Malaysian natural rubber. Rubber material is chosen because it has very high damping to ensure the sufficient dissipation of vibration energy from the seismic wave. They are two methods involve in this paper, which are lumped parameter and wave propagation techniques. The lumped parameter system is developed to represent the baseline model of laminated rubber-metal spring. Wave propagation model is developed using non-dispersive rod. The mathematical modeling of laminated rubber-metal spring has been developed based on the internal resonance, lumped parameter and finite rod model, respectively. For a conclusion, the mathematical modeling of a prediction of basic and circular vibration isolator can be as a tool to predict the new trial-error method for developing new compounding of the vibration isolator in future, respectively.

Keywords: Laminated rubber-metal spring, vibration isolator, Malaysian natural rubber, internal resonance, transmissibility

1. INTRODUCTION

Currently, there are over 3500 articles discussing the role of the vibration isolators in dissipating energy, by considering various combinations of restoring and damping forces applied on the system. Harrison had developed an exact solution for vibratory response called symmetric system, which consisted of coulomb and viscous damping [1]. Both damping's were subjected to a harmonic motion. Then, Ruzicka and Derby created and analysed the extensive results for vibration isolator systems due to linear stiffness [2]. Based on these two studies, the magnitude of stiffness required in designing the new vibration isolators had been found and transmissibility force could be predicted by referring to the resonant amplitudes. Hundal and Parnes (1979) conducted an experiment by using the same system subjected to base excitation in 1979.

*Corresponding Author: azli@utem.edu.my

Then, in 1990, Nayfah developed passive mechanical vibration isolator consisting of discrete mass, stiffness, and damping elements [3]. This system was similar to lumped parameter system and it was discovered that the effectiveness of the vibration isolators was when subjected to a harmonic excitation in certain frequency ranges. The resonances of the isolator were similar compared to the previous researches and the level of transmitted force was further reduced [4]. The new design of vibration isolators is needed to increase the performance of the isolator by shifting the resonance frequency, thus increases the effectiveness of the isolator. But the problem is come when the vibration isolator need to performance in high frequencies.

To do so, this paper aim to develop and modify the existing vibration isolator which is create by conventional lumped parameter system to new system, namely as discrete lumped parameter system. Based on this new system, it hopes can be used to design new vibration isolator that can perform better and good response in higher frequencies phenomenon.

2. MODELLING OF DISCRETE LUMPED PARAMETER SYSTEM

The development of the discrete lumped parameter system which is adopted from the conventional lumped parameter system. Additionally, the intention is to break the isolator into discrete springs and masses to take into account the effect of inertial mass. The distributed mass is assumed to have total mass equivalent to the mass of the isolator, and the stiffness value is according to the height of the isolator and based on the value of the overall stiffness from the isolator. The excitation force F_e, transmitted force F_t and, finally, displacement u were used in this system [5-7].

The benchmarking to develop the discrete lumped parameter system is taken from the distributed parameter isolator model. Figure 1 shows the modified distributed parameter isolator compared to the discrete lumped parameter system.

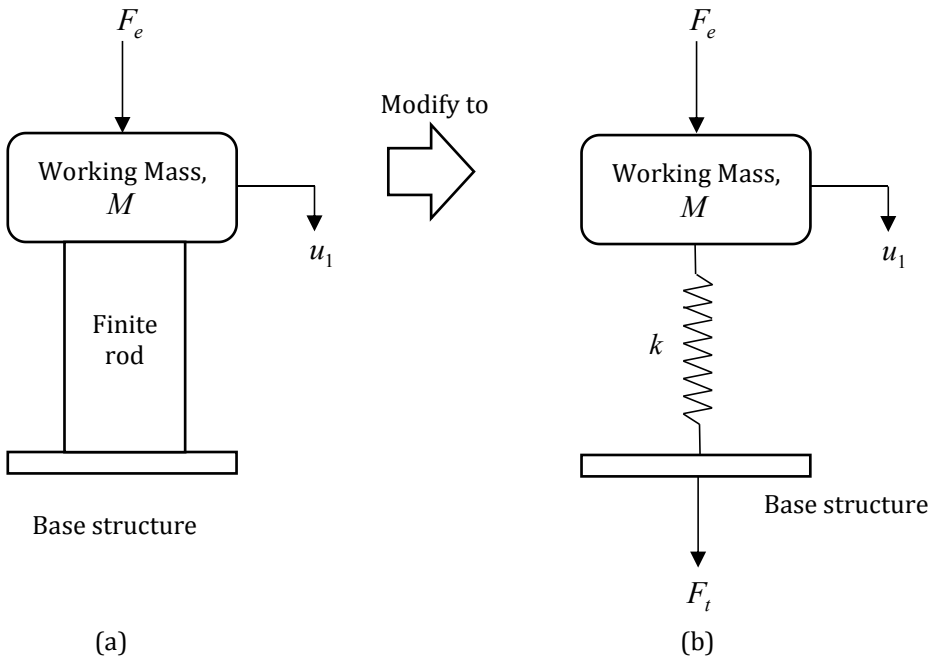

Figure 1. Discrete lumped parameter systems
(a) distributed parameter isolator and (b) discrete lumped parameter system.

The equation of motion for the discrete lumped parameter system can be given as

$$F_e = M\ddot{u}_1 + ku_1 \tag{1}$$

and

$$F_t = ku_1 \tag{2}$$

In harmonic motion, both equations of motion in Eqs. (1) and (2) become

$$F_e = -\omega^2 MU_1 + kU_1 \tag{3}$$

and

$$F_t = kU_1 \tag{4}$$

where, U is the complex amplitude, ω is the frequency, F_e is excitation force and F_t is transmitted force.

By referring back to Eq. (3.38), the general transmissibility equation is

$$T_r = \left| \frac{F_t}{F_e} \right| \tag{5}$$

By inserting Eqs. (3) and (4) into (5), the transmissibility equation for the single-degree-of-freedom for the discrete lumped parameter system can be given as

$$T_r = \left| \frac{kU_1}{-\omega^2 MU_1 + kU_1} \right| \tag{6}$$

By comparing Eq. (3.112) with the transmissibility equations for the single-degree-of-freedom for impedance and stiffness for the LR-MS model.

Therefore, the previous steps to derive the discrete lumped parameter system can be used in developing the higher-degree-of-freedom of the system in this section.

2.1 Multi-Degree-of-Freedom

In this section, the multi-degree-of-freedom of the discrete lumped parameter system is discussed, and the aim is to develop the internal resonance behaviour to be the same as inside the distributed parameter isolator system. For the two-degree-of-freedom discrete lumped parameter system, the rubber was divided into two spring elements. However, additionally, the total value of stiffness remained the same as the stiffness value in the single-degree-of-freedom system and also the mass of the rubber remains the same. Figure 2 illustrates the schematic diagram for the two-degree-of-freedom discrete lumped parameter system.

The equations of motion for the systems can be derived as

$$F_e = M\ddot{u}_1 + \frac{k}{2}u_1 - \frac{k}{2}u_2 \tag{7}$$

$$0 = m\ddot{u}_2 + \frac{k}{2}u_2 - \frac{k}{2}u_1 \tag{8}$$

and

$$F_t = \frac{k}{2}u_2 \tag{9}$$

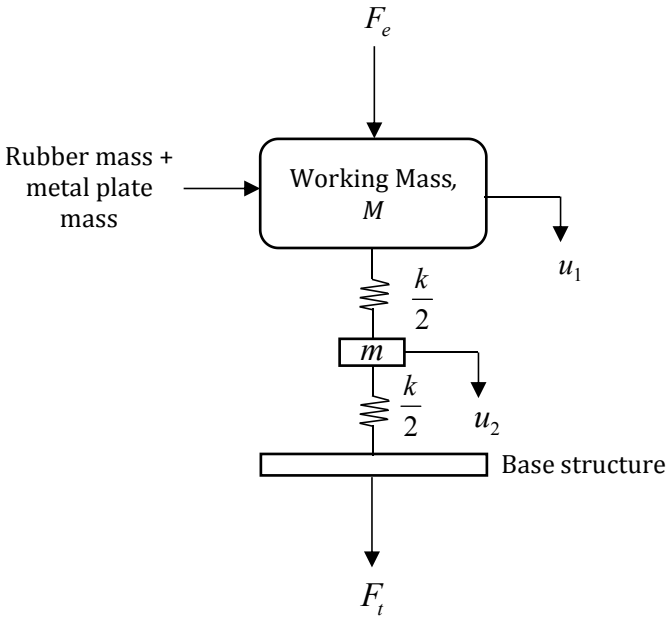

Figure 2. Two-degree-of-freedom discrete lumped parameter system.

In harmonic motion, Eqs. (7) to (9) become

$$F_e = -\omega^2 MU_1 + \frac{k}{2}U_1 - \frac{k}{2}U_2 \tag{10}$$

$$0 = -\omega^2 mU_2 + \frac{k}{2}U_2 - \frac{k}{2}U_1 \tag{11}$$

and

$$F_t = \frac{k}{2}U_2 \tag{12}$$

By simplifying Eqs. (10) and (11), the new equations are given by

$$F_e = \left(\frac{k}{2} - \omega^2 M\right)U_1 - \frac{k}{2}U_2 \tag{13}$$

and

$$0 = \left(\frac{2k}{2} - \omega^2 m\right)U_2 - \frac{k}{2}U_1 \tag{14}$$

By taking U_2 as a reference for U_1, therefore Eq. (14) can be written and then simplified as

$$U_1 = \left(2 - \frac{2}{k}\omega^2 m\right) U_2 \tag{15}$$

Then, to solve Eq. (3.119), Eq. (3.121) is used, and, finally, the new equation becomes

$$F_e = \left(\frac{k}{2} - \omega^2 M\right)\left(2 - \frac{2}{k}\omega^2 m\right) U_2 - \frac{k}{2} U_2 \tag{16}$$

By again taking the transmissibility equation for the two-degree-of-freedom discrete lumped parameter into the isolator, is given by

$$T_r = \left|\frac{F_t}{F_e}\right| = \left|\frac{\frac{k}{2} U_2}{\left(\frac{k}{2} - \omega^2 M\right)\left(2 - \frac{2}{k}\omega^2 m\right) U_2 - \frac{k}{2} U_2}\right| \tag{17}$$

For the three-degree-of-freedom discrete lumped parameter system, the stiffness value was divided into three parts of spring element and the mass of the rubber was divided into two. However, the total mass was equivalent to the total mass of the two-degree-of-freedom discrete lumped parameter system. Figure 3 shows the schematic diagram of the system. Then, the equation of motion of this system can be given as

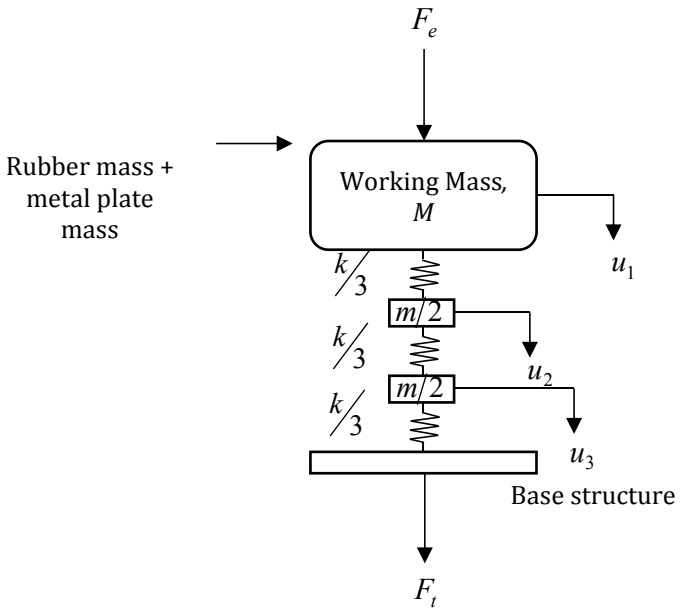

Figure 3. Three-degree-of-freedom discrete lumped parameter system.

$$F_e = M\ddot{u}_1 + \frac{k}{3}u_1 - \frac{k}{3}u_2 \tag{18}$$

$$0 = \frac{m}{2}\ddot{u}_2 + \frac{2k}{3}u_2 - \frac{k}{3}u_1 - \frac{k}{3}u_3 \tag{19}$$

$$0 = \frac{m}{2}\ddot{u}_3 + \frac{2k}{3}u_3 - \frac{k}{3}u_2 \tag{20}$$

and

$$F_t = \frac{k}{3}u_3 \tag{21}$$

For harmonic motion, then Eqs. (18) to (21) become

$$F_e = -\omega^2 M U_1 + \frac{k}{3}U_1 - \frac{k}{3}U_2 \tag{22}$$

$$0 = -\omega^2 \frac{m}{2}U_2 + \frac{2k}{3}U_2 - \frac{k}{3}U_1 - \frac{k}{3}U_3 \tag{23}$$

$$0 = -\omega^2 \frac{m}{2}U_3 + \frac{2k}{3}U_3 - \frac{k}{3}U_2 \tag{24}$$

and

$$F_t = \frac{k}{3}U_3 \tag{25}$$

By simplifying Eqs. (22) to (24), the equations are written as

$$F_e = \left(\frac{k}{3} - \omega^2 M\right)U_1 - \frac{k}{3}U_2 \tag{26}$$

$$0 = \left(\frac{2k}{3} - \omega^2 \frac{m}{2}\right)U_2 - \frac{k}{3}U_1 - \frac{k}{3}U_3 \tag{27}$$

and

$$0 = \left(\frac{2k}{3} - \omega^2 \frac{m}{2}\right)U_3 - \frac{k}{3}U_2 \tag{28}$$

By taking U_3 as a reference of U_2, therefore, the new equation can be derived as

$$U_2 = \left(2 - 3\omega^2 \frac{m}{k}\right)U_3 \tag{29}$$

On the other hand, from Eq. (27), U_2 and U_1 can be written as a reference for U_3. After rearranging the equation, finally, it can be given as

$$U_3 = \left(2k^2 - \frac{3}{2}\omega^2 mk\right)U_2 - k^2 U_1 \tag{30}$$

By substituting Eq. (30) into Eq. (29), the equation can be written as

$$U_2 = \frac{-k^2}{1-\left(2-3\omega^2\frac{m}{k}\right)\left(2k^2-\frac{3}{2}\omega^2 mk\right)}U_1 \tag{31}$$

Then, by inserting Eq. (29) into Eq. (31), the equation is become

$$\left(2-3\omega^2\frac{m}{k}\right)U_3 =_2= \frac{-k^2}{1-\left(2-3\omega^2\frac{m}{k}\right)\left(2k^2-\frac{3}{2}\omega^2 mk\right)}U_1 \tag{32}$$

By simplifying Eq. (32), it can be written as

$$U_1 = \frac{\left(2-3\omega^2\frac{m}{k}\right)U_3 \times \left[1-\left(2-3\omega^2\frac{m}{k}\right)\left(2k^2-\frac{3}{2}\omega^2 mk\right)\right]}{-k^2} \tag{33}$$

Then, by substituting Eqs. (29) and (33) into Eq. (26), the equation is become

$$F_e = \left(\frac{k}{3}-\omega^2 M\right)\times\frac{\left(2-3\omega^2\frac{m}{k}\right)U_3 \times \left[1-\left(2-3\omega^2\frac{m}{k}\right)\left(2k^2-\frac{3}{2}\omega^2 mk\right)\right]}{-k^2} - \frac{k}{3}\left(2-3\omega^2\frac{m}{k}\right)U_3 \tag{34}$$

By simplifying Eq. (34), the equation of excitation force becomes

$$F_e = \left(\frac{k}{3}-\omega^2 M\right)\left(2-\frac{3}{k}\omega^2 m\right)U_3 - \frac{k}{3}U_3 \tag{35}$$

Therefore, the transmissibility equation of the three-degree-of-freedom discrete lumped parameter system can be written as

$$T_r = \left|\frac{F_t}{F_e}\right| = \left|\frac{\frac{k}{3}U_3}{\left(\frac{k}{3}-\omega^2 M\right)\left(2-\frac{3}{k}\omega^2 m\right)U_3 - \frac{k}{3}U_3}\right| \tag{36}$$

Then, by dividing into three parts of the rubber mass, and dividing the stiffness into four parts of spring elements, the system is represented as four-degree-of-freedom discrete lumped parameter system. However, the total value for stiffness and mass of rubber remained equivalent compared to the previous system. Figure 4 shows the schematic diagram of the system. The equations of motion for the system are written below.

$$F_e = M\ddot{u}_1 + \frac{k}{4}u_1 - \frac{k}{4}u_2 \tag{37}$$

$$0 = \frac{m}{3}\ddot{u}_2 + \frac{2k}{4}u_2 - \frac{k}{4}u_1 - \frac{k}{4}u_3 \tag{38}$$

$$0 = \frac{m}{3}\ddot{u}_3 + \frac{2k}{4}u_3 - \frac{k}{4}u_2 - \frac{k}{4}u_4 \tag{39}$$

$$0 = \frac{m}{3}\ddot{u}_4 + \frac{2k}{4}u_4 - \frac{k}{4}u_3 \tag{40}$$

and

$$F_t = \frac{k}{4}u_4 \tag{41}$$

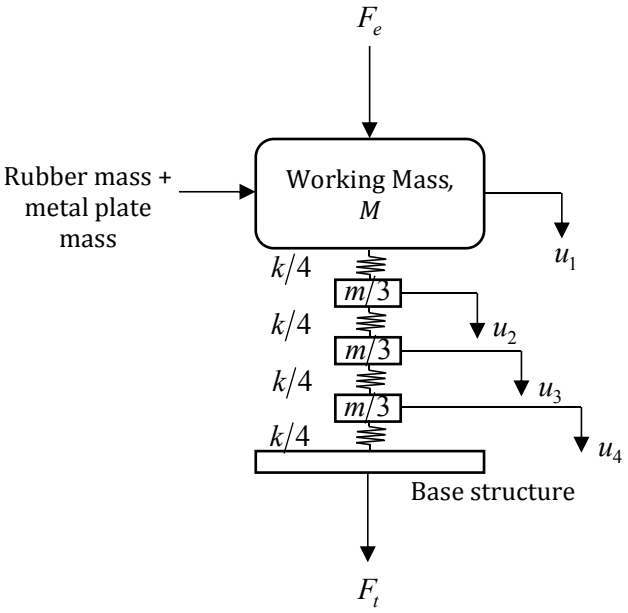

Figure 4. Four-degree-of-freedom discrete lumped parameter system.

Then, in harmonic motion, the equations of motion become

$$F_e = -\omega^2 M U_1 + \frac{k}{4}U_1 - \frac{k}{4}U_2 \tag{42}$$

$$0 = -\omega^2 \frac{m}{3}U_2 + \frac{2k}{4}U_2 - \frac{k}{4}U_1 - \frac{k}{4}U_3 \tag{43}$$

$$0 = -\omega^2 \frac{m}{3}U_3 + \frac{2k}{4}U_3 - \frac{k}{4}U_2 - \frac{k}{4}U_4 \tag{44}$$

$$0 = -\omega^2 \frac{m}{3}U_4 + \frac{2k}{4}U_4 - \frac{k}{4}U_3 \tag{45}$$

and

$$F_t = \frac{k}{4}U_4 \tag{46}$$

By simplifying Eqs. (42) to (43), the equations are given by

$$F_e = \left(\frac{k}{4} - \omega^2 M\right) U_1 - \frac{k}{4} U_2 \tag{47}$$

$$0 = \left(\frac{2k}{4} - \omega^2 \frac{m}{3}\right) U_2 - \frac{k}{4} U_1 - \frac{k}{4} U_3 \tag{48}$$

$$0 = \left(\frac{2k}{4} - \omega^2 \frac{m}{3}\right) U_3 - \frac{k}{4} U_2 - \frac{k}{4} U_4 \tag{49}$$

and

$$0 = \left(\frac{2k}{4} - \omega^2 \frac{m}{3}\right) U_4 - \frac{k}{4} U_3 \tag{50}$$

From Eq. (49), U_3 and U_4 can be written as a reference for U_2. Therefore, by rearranging the equation, it then becomes

$$U_2 = \left(2k^2 - 4\omega^2 \frac{m}{3} k\right) U_3 - k^2 U_4 \tag{51}$$

By rearranging Eq. (49), and letting U_3 be a reference value of U_4, finally, the equation can be expressed as

$$U_4 = \frac{k}{4}\left(\frac{1}{\frac{2k}{4} - \omega^2 \frac{m}{3}}\right) U_3 \tag{52}$$

By substituting Eq. (52) into Eq. (51), it gives

$$U_2 = \left(2k^2 - 4\omega^2 \frac{m}{3} k\right) U_3 - k_2 \left[\frac{k}{4}\left(\frac{1}{\frac{2k}{4} - \omega^2 \frac{m}{3}}\right)\right] U_3 \tag{53}$$

By inserting Eq. (53) into Eq. (49), then the equation becomes

$$0 = \left(\frac{2k}{4} - \omega^2 \frac{m}{3}\right) U_3 - \frac{k}{4}\left(2k^2 - 4\omega^2 \frac{m}{3} k\right) U_3 - k_2 \left[\frac{k}{4}\left(\frac{1}{\frac{2k}{4} - \omega^2 \frac{m}{3}}\right)\right] U_3 - \frac{k}{4} U_4 \tag{54}$$

By rearranging Eq. (51), the equation becomes

$$U_3 = \frac{U_2 + k^2 U_4}{2k^2 - 4\omega^2 \frac{m}{3} k} \tag{55}$$

By inserting Eq. (55) into Eq. (54), the equation can be written as

$$0=\left[\left(\frac{2k}{4}-\omega^2\frac{m}{3}\right)\times\left(\frac{U_2+k^2U_4}{2k^2-4\omega^2\frac{m}{3}k}\right)\right]-\left[\frac{k}{4}\left(2k^2-4\omega^2\frac{m}{3}k\right)\times\left(\frac{U_2+k^2U_4}{2k^2-4\omega^2\frac{m}{3}k}\right)\right]\ldots$$

$$\ldots-k_2\left[\frac{k}{4}\left(\frac{1}{\frac{2k}{4}-\omega^2\frac{m}{3}}\right)\times\left(\frac{U_2+k^2U_4}{2k^2-4\omega^2\frac{m}{3}k}\right)\right]-\frac{k}{4}U_4 \tag{56}$$

By dividing Eq. (56) into small group, there are become

$$G1=\left(\frac{2k}{4}-\omega^2\frac{m}{3}\right)\times\left(\frac{U_2+k^2U_4}{2k^2-4\omega^2\frac{m}{3}k}\right) \tag{57}$$

$$G2=\frac{k}{4}\left(2k^2-4\omega^2\frac{m}{3}k\right)\times\left(\frac{U_2+k^2U_4}{2k^2-4\omega^2\frac{m}{3}k}\right) \tag{58}$$

$$G3=k_2\left[\frac{k}{4}\left(\frac{1}{\frac{2k}{4}-\omega^2\frac{m}{3}}\right)\times\left(\frac{U_2+k^2U_4}{2k^2-4\omega^2\frac{m}{3}k}\right)\right] \tag{59}$$

and

$$G4=\frac{k}{4}U_4 \tag{60}$$

By substituting Eq. (55) into Eq. (48), the equation can be expressed as

$$0=\left(\frac{2k}{4}-\omega^2\frac{m}{3}\right)U_2-\frac{k}{4}U_1-\frac{k}{4}\left(\frac{U_2+k^2U_4}{2k^2-4\omega^2\frac{m}{3}k}\right) \tag{61}$$

By simplifying Eq. (61), the equation is become

$$U_2 = \frac{\left(\frac{k^3 U_4}{8k^2 - 16\omega^2 \frac{m}{3}k}\right) - \frac{k}{4}U_1}{\left(\frac{2k}{4} - \frac{\omega^2 m}{3}\right) - \left(\frac{1}{8k^2 - 16\omega^2 \frac{m}{3}k}\right)} \tag{62}$$

By inserting Eq. (62) into Eqs. (60) to (59), the equations are becoming

$$G1 = \left(\frac{2k}{4} - \omega^2 \frac{m}{3}\right) \times \frac{\left(\frac{k^3 U_4}{8k^2 - 16\omega^2 \frac{m}{3}k}\right) - \frac{k}{4}U_1}{\left(\frac{2k}{4} - \frac{\omega^2 m}{3}\right) - \left(\frac{1}{8k^2 - 16\omega^2 \frac{m}{3}k}\right)} + k^2 U_4 \times \left(\frac{1}{2k^2 - 4\omega^2 \frac{m}{3}k}\right) \tag{63}$$

$$G2 = \frac{k}{4}\left(2k^2 - 4\omega^2 \frac{m}{3}k\right) \times \frac{\left(\frac{k^3 U_4}{8k^2 - 16\omega^2 \frac{m}{3}k}\right) - \frac{k}{4}U_1}{\left(\frac{2k}{4} - \frac{\omega^2 m}{3}\right) - \left(\frac{1}{8k^2 - 16\omega^2 \frac{m}{3}k}\right)} + k^2 U_4 \times \left(\frac{1}{2k^2 - 4\omega^2 \frac{m}{3}k}\right) \tag{64}$$

and

$$G3 = k_2 \left[\frac{k}{4}\left(\frac{1}{\frac{2k}{4} - \omega^2 \frac{m}{3}}\right) \times \frac{\left(\frac{k^3 U_4}{8k^2 - 16\omega^2 \frac{m}{3}k}\right) - \frac{k}{4}U_1}{\left(\frac{2k}{4} - \frac{\omega^2 m}{3}\right) - \left(\frac{1}{8k^2 - 16\omega^2 \frac{m}{3}k}\right)} + k^2 U_4 \times \left(\frac{1}{2k^2 - 4\omega^2 \frac{m}{3}k}\right)\right] \tag{65}$$

By simplified the Eqs. (63) to (65), and then inserting the simplifying group into Eq. (3.162), and finally transferring the equation into Eq. (47), the excitation force equation is become

$$F_e = \left(\frac{k}{4} - \omega^2 M\right)\left(2 - \frac{4}{k}\omega^2 m\right)U_4 - \frac{k}{4}U_4 \tag{66}$$

Finally, the transmissibility equation for four-degree-of-freedom discrete lumped parameter system can be written as follows

$$T_r = \left|\frac{F_t}{F_e}\right| = \left|\frac{\frac{k}{4}U_4}{\left(\frac{k}{4}-\omega^2 M\right)\left(2-\frac{4}{k}\omega^2 m\right)U_4 - \frac{k}{4}U_4}\right| \tag{67}$$

By observing Eqs. (15), (16), (17) and (67), it can be seen that there is a relationship regarding the pattern of the transmissibility equation for two-degree-of-freedom discrete lumped parameter system and onwards. However, it is very hard to derive the discrete lumped parameter system by dividing the mass of rubber at higher number. The general equation of discrete lumped parameter system for higher-degree-of-freedom can be represented as

$$T_r = \left|\frac{F_t}{F_e}\right| = \left|\frac{\frac{k}{N}U_N}{\left(\frac{k}{N}-\omega^2 M\right)\left(2-\frac{N}{k}\omega^2 m\right)U_N - \frac{k}{N}U_N}\right| \tag{68}$$

where N is a number of degree-of-freedom of discrete lumped parameter system.

The working mass M used in this system has the same weight as the previous working mass used in the LR-MS model and also in the conventional lumped parameter system. Additionally, the stiffness value for the discrete lumped parameter system was obtained from the stiffness value of the non-dispersive finite rod. This value is taken because it needs to give the same stiffness value between the LR-MS model and discrete lumped parameter system, particularly.

All of the transmissibility equations for the discrete lumped parameter system are used again, and then the transmissibility results are plotted, and, finally, they are compared with the conventional lumped parameter system and additionally with the LR-MS model results.

3. RESULTS AND DISCUSSION

3.1 Multi-Degree-of-Freedom

Figure 5 shows the comparison results between the single-degree-of-freedom conventional lumped parameter system and the discrete lumped parameter system, particularly. The natural frequency for each graph remained at 10 Hz because used the same properties, and the graphs went below unity. The roll-off rate for the discrete lumped parameter system was recorded at 20 dB per decade, and it was similar to the roll-off rate that was captured in the conventional lumped parameter system and shown in Figure 6.

Additionally, the comparison results between the discrete lumped parameter system and the LR-MS model for the single-degree-of-freedom system are illustrated in Figure 6. In contrast, both results indicate that the natural frequency was placed at approximately 10 Hz. The second peak (internal resonance start) for the LR-MS model was obtained; however, in the single-degree-of-freedom discrete lumped parameter system, the second peak did not appear. This happened because it only has one mass, called working mass [8-9]. This mass only occurs when the excitation force excites the system, and, finally, the working mass influenced the natural frequency result.

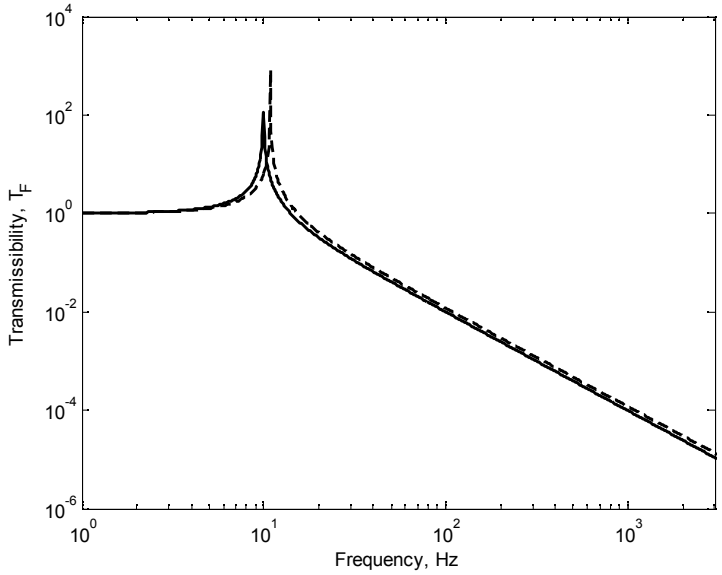

Figure 5. Result for single-degree-of-freedom
(——: conventional and ----: discrete lumped parameter system).

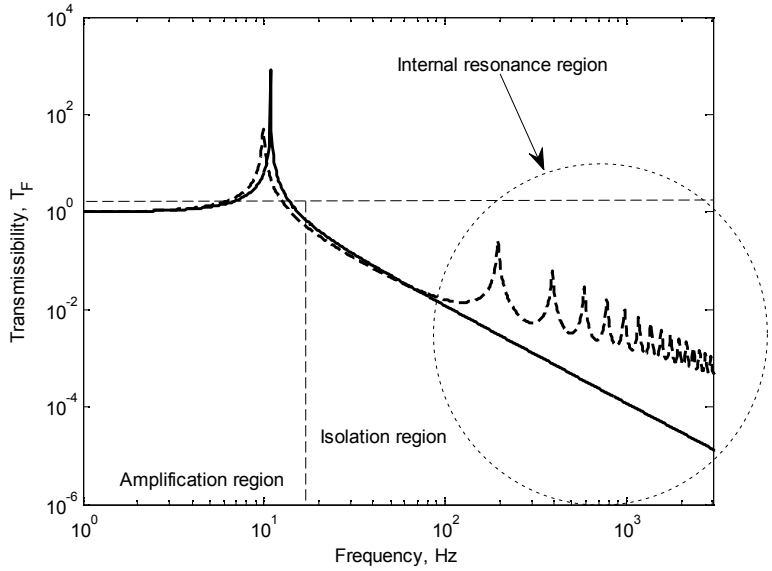

Figure 6. Comparison results for LR-0MS
(---: LR-0MS model and——: single-degree-of-freedom discrete lumped parameter system).

Figure 7 shows the comparison results between the two-degree-of-freedom discrete lumped parameter system and the LR-1MS model. The first natural frequency for both graphs remained at 10 Hz; however, the second natural frequency did not. The second natural frequency for the discrete lumped parameter system is 150 Hz away from the location of the second natural frequency of the LR-1MS model. The result for the three-degree-of-freedom discrete lumped parameter system is shown in Figure 8, with a comparison between it and the LR-2MS model. The first natural frequency remains at 10 Hz, but the second and third natural frequencies of the discrete lumped parameter system went far away from the location of the second and third natural frequencies of the LR-2MS model. However, the position of the second natural frequency of the discrete lumped parameter system is lower than compared to its position in the previous

system (by adding a single metal plate to the discrete lumped parameter system), and the decrease is recorded at 42 Hz.

Then, for the four-degree-of-freedom discrete lumped parameter system, the transmissibility equation can be referred to at Eq. (61). Figure 9 shows the comparison results between the discrete lumped parameter system with three metal plates and the LR-3MS model. Like the previous system, the first natural frequency is located at 10 Hz, but, the second, third and fourth natural frequencies are located at different positions, but the positions decreased by up to 60 Hz for the second natural frequency and 23 Hz for the third natural frequency, particularly, when comparing the results in Figure 6. By using this pattern, it is believed that, by increasing the number of metal plates [10-11], the second natural frequency, etc., in the lumped parameter system will be located near to the second natural frequency, etc., of the LR-MS system.

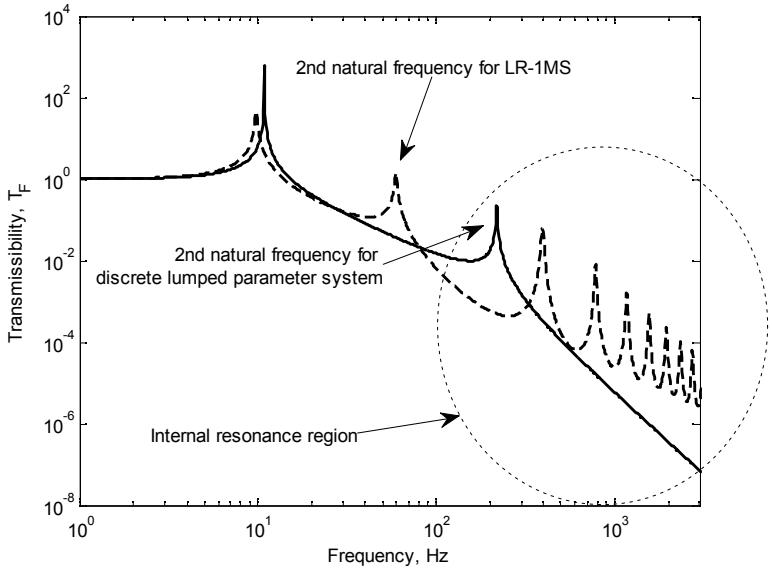

Figure 7. Comparison results for LR-1MS
(---: LR-1MS model and ——: two-degree-of-freedom discrete lumped parameter system).

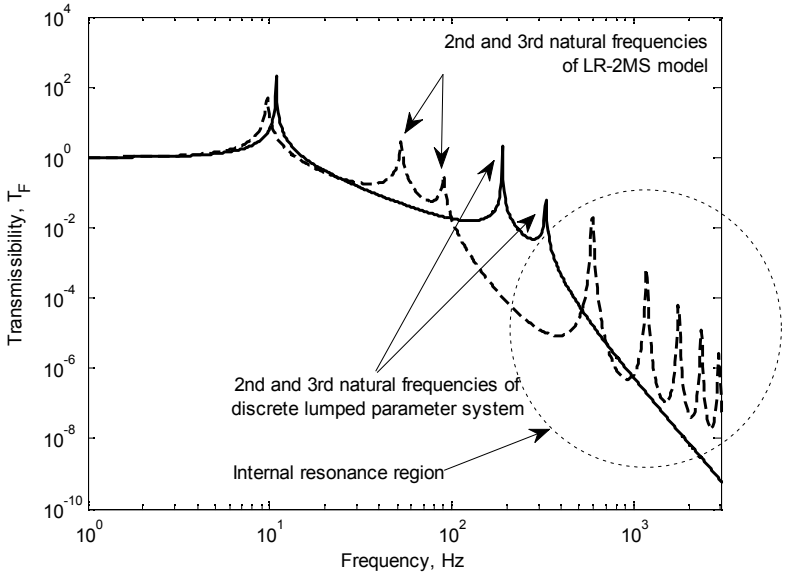

Figure 8. Comparison results for LR-2MS
(---: LR-2MS model and ——: three-degree-of-freedom discrete lumped parameter system).

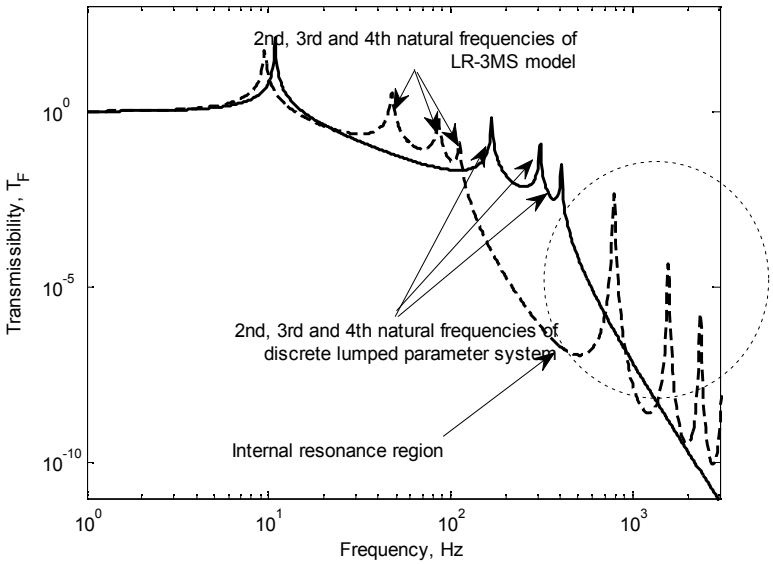

Figure 9. Comparison results for LR-3MS
(---: LR-3MS model and ── : four-degree-of-freedom discrete lumped parameter system).

3.2 Higher-Degree-of-Freedom

The numerical software was used to derive the excitation force of the discrete lumped parameter system when dividing higher number of original rubber mass. Figures 10 to 12 show the results when dividing the mass of rubber into eight parts. The natural frequency for each graph remained at 10 Hz, and then the graphs went below unity. However, at 900 Hz, the graph of the discrete lumped parameter system increased and was close to unity, where the peaks were obtained at 1380 Hz, and, finally, it refrained until the end of the graph. Additionally, this only occurred at high frequencies. The roll-off rate for the discrete lumped parameter system was recorded at 20 dB per decade, and it was similar to the roll-off rate that was captured in the conventional lumped parameter system. In addition, in the discrete lumped parameter system, this second natural frequency also can be recognized as a first peak of the internal resonance, and it will be used as an indicator to investigate the vibration performance in future.

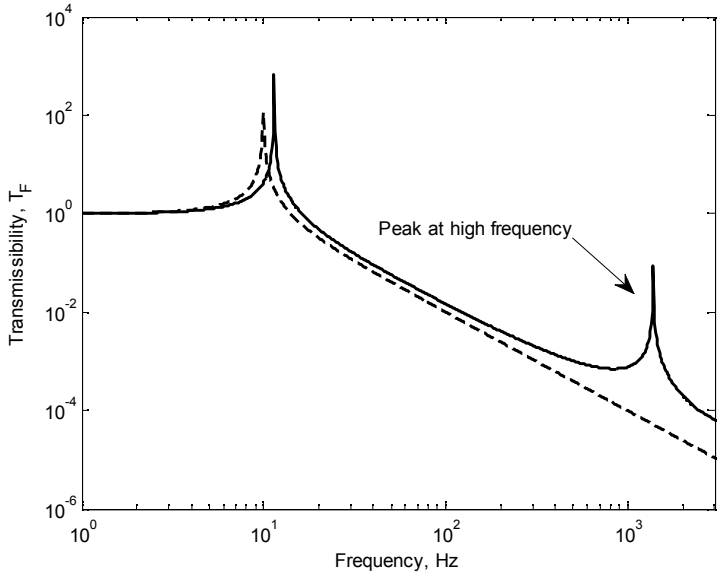

Figure 3.10. Result for Dividing Rubber Mass into 8 parts (Conventional)
(---: conventional and ──: discrete lumped parameter system).

A discussion then followed to investigate the wave effect in both systems. It explored several characteristic lines in the transmissibility results. Additionally, the crossing point also appeared when both results were plotted in the same graph. Theoretically, all of these characteristic points were discussed in detail, and Figure 12 shows the characteristics for the discrete lumped parameter system (dividing rubber mass into eight parts) and LR-MS model.

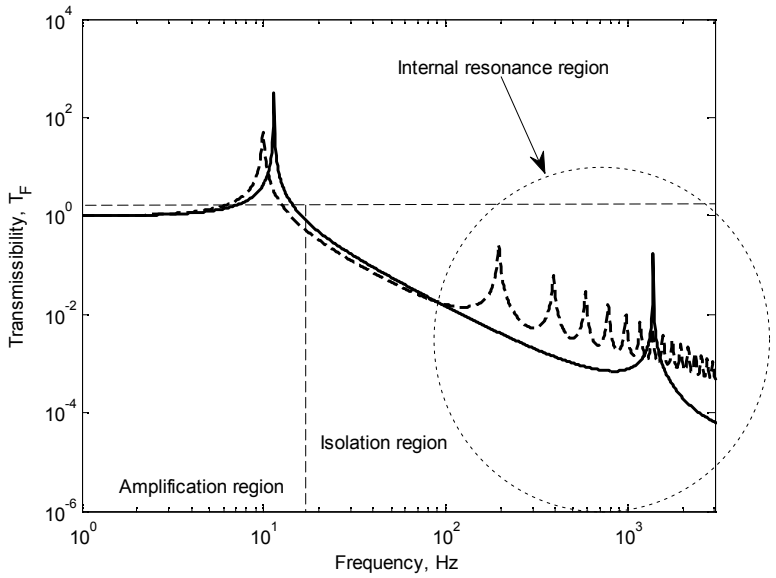

Figure 11. Result for dividing rubber mass into 8 parts
(---: LR-MS model and ——: discrete lumped parameter system).

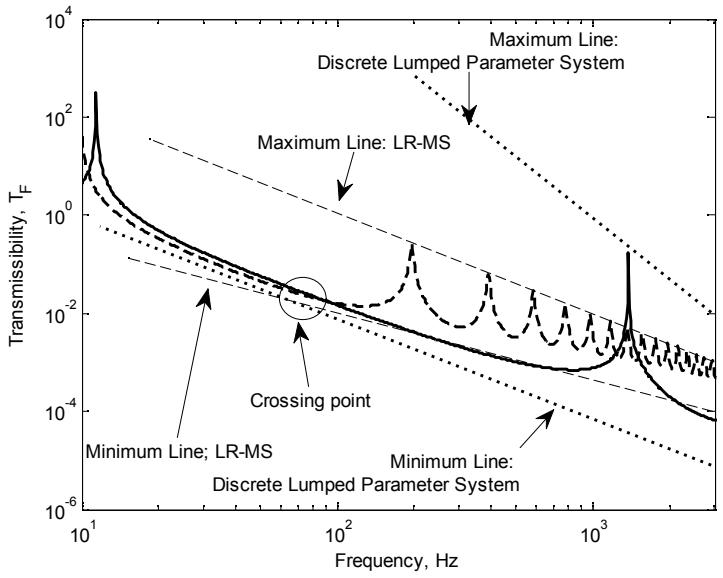

Figure 12. Characteristic lines for dividing rubber mass into 8 parts
(---: LR-MS model and —— : discrete lumped parameter system).

By dividing it into 12 parts, the first and second natural frequencies of the discrete lumped parameter system are positioned near to the natural frequencies of the LR-1MS model. Figure 13 shows the comparison graph for both systems. Additionally, a third peak appeared, and it was positioned at the middle of the internal resonance positioning of the LR-1MS model. It is

believed that it is an internal resonance peak of the discrete lumped parameter system. Then, Figure 14 shows the characteristic lines of the system.

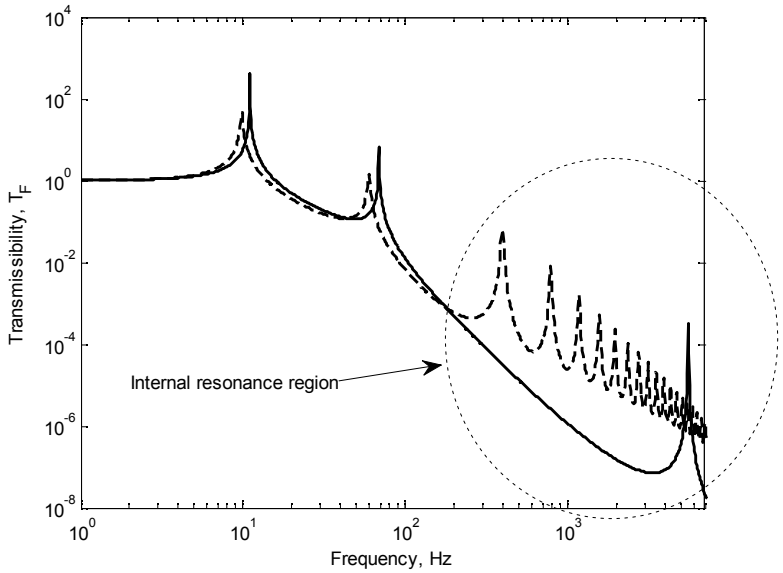

Figure 13. Result for dividing rubber mass into 12 parts
(---: LR-1MS model and —— : discrete lumped parameter system).

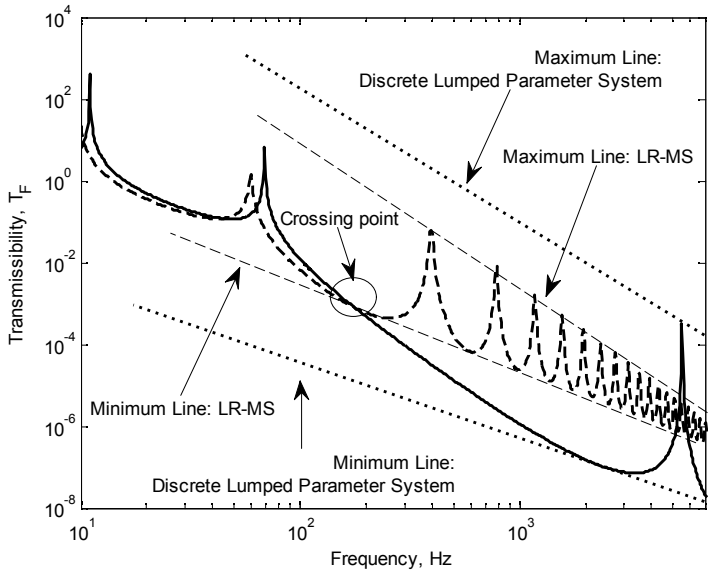

Figure 14. Characteristic lines for dividing rubber mass into 12 parts
(---: LR-1MS model and —— : discrete lumped parameter system).

This graph pattern was continued by increasing up to 16 parts inside the discrete lumped parameter system. All of the natural frequencies in this system which are positioned near to the natural frequencies have been recorded at the LR-2MS model. Then, a fourth peak appeared, and the positioning is the same as in the previous system, which is located at the centre of the internal resonance of the LR-2MS model. The result is shown in Figure 15 and then Figure 16 shows the characteristic lines, particularly.

The results after dividing the rubber mass into 20 parts are shown in Figures 17 and 18. Finally, Figures 19 to 21 show the results when dividing the rubber mass into 32, 41 and 68 parts. The

first natural frequency for all graphs remained at 10 Hz. For division into 41 parts, the second natural frequency positioning is near to that of the LR-1MS model, and then, for division into 68 parts, the second and third natural frequencies are located near to those in the LR-2MS model. Based on the results, it can be seen that the internal resonance peaks for the discrete lumped parameter system have appeared at high frequencies.

Additionally, the internal resonance peak at the discrete lumped parameter system was greater for the LR-MS model. This occurred because, in the discrete lumped parameter system, only the stiffness was taken into account to analyse the transmissibility, and also zero damping was presumed. According to the sliding point (the graph went far from unity) in the isolation region, the discrete lumped parameter system was going far away from unity due to frequency increases. Therefore, the LR-MS model was the better model to investigate the performance of the vibration isolator, but, on the other hand, the discrete lumped parameter can be used as a reference point to compare the results in future.

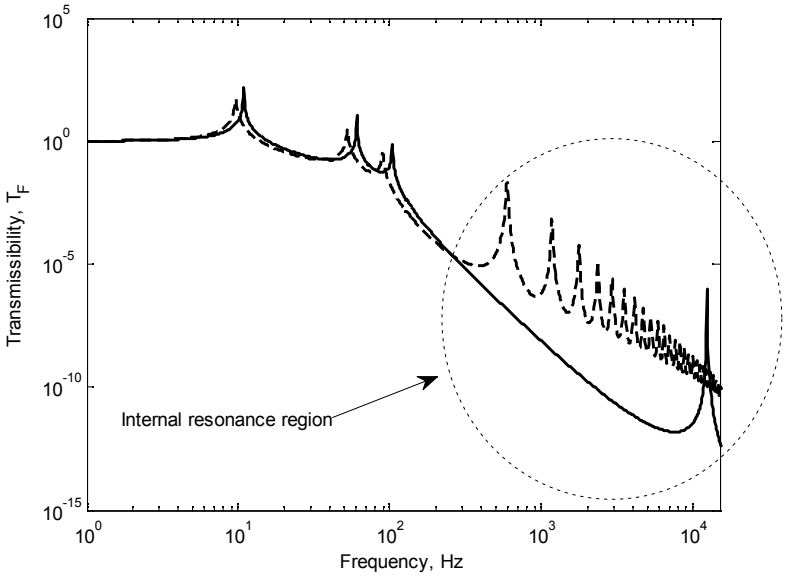

Figure 15. Result for dividing rubber mass into 16 parts
(---: LR-2MS model and ── : discrete lumped parameter system).

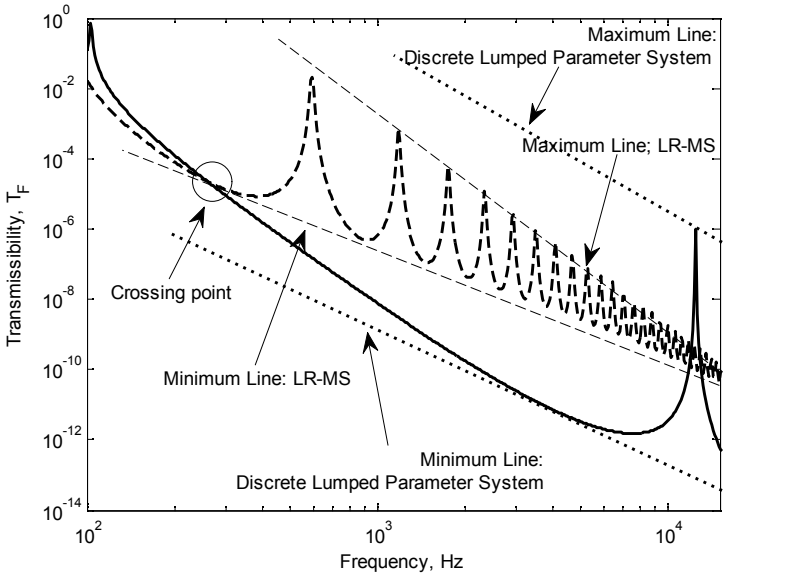

Figure 16. Characteristic lines for dividing rubber mass into 16 parts
(---: LR-2MS model and ── : discrete lumped parameter system).

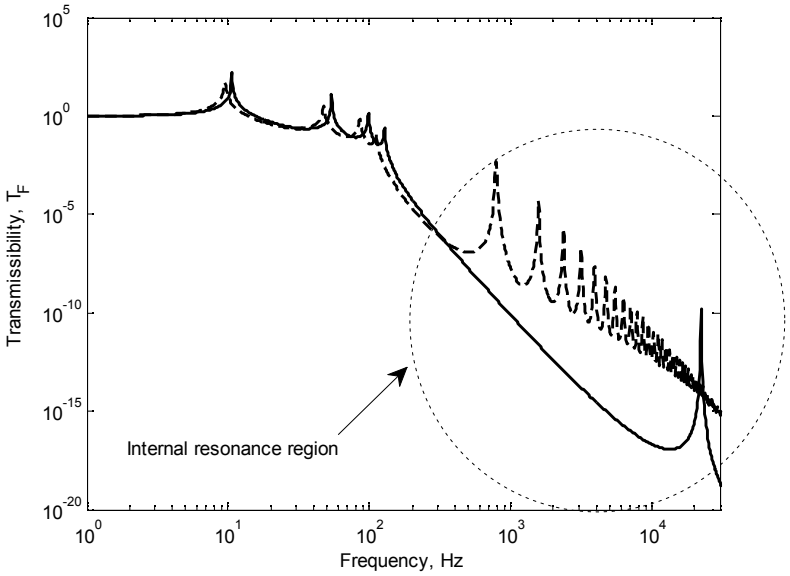

Figure 17. Result for Dividing Rubber Mass into 20 Parts
(---: LR-3MS Model and ——: Discrete Lumped Parameter System).

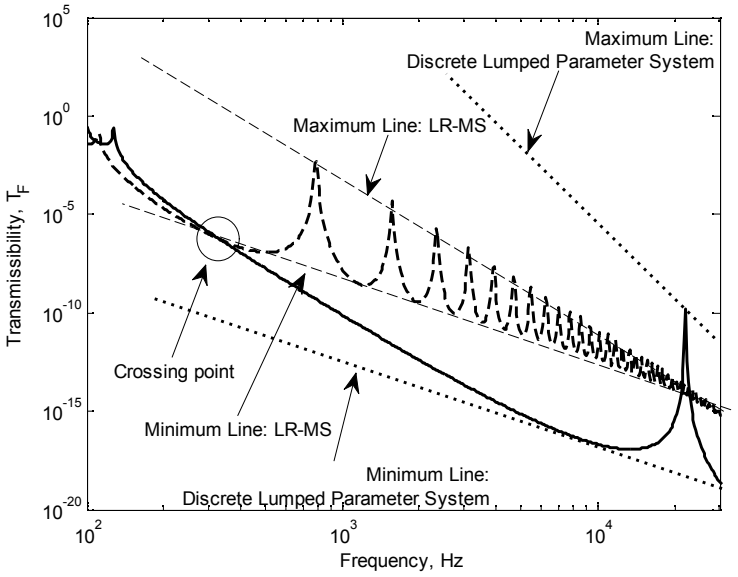

Figure 18. Characteristic lines for dividing rubber mass into 20 parts
(---: LR-3MS model and ——: discrete lumped parameter system).

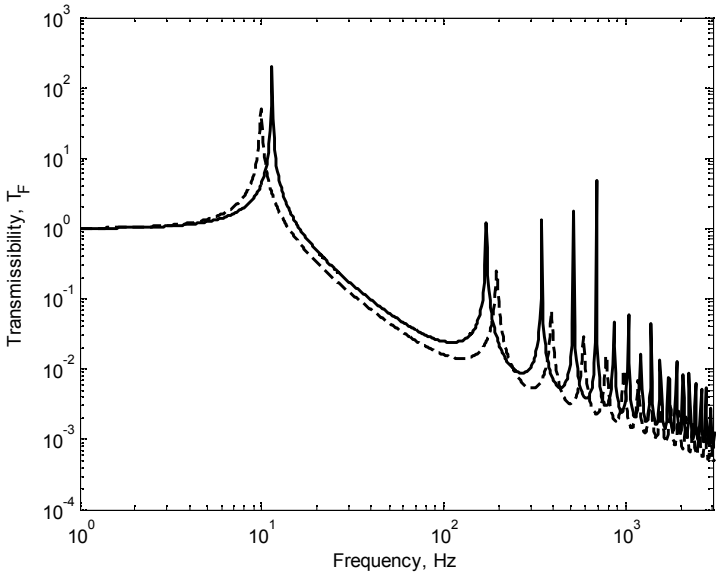

Figure 19. Result for dividing rubber mass into 32 parts
(---: LR-MS model and ——: discrete lumped parameter system).

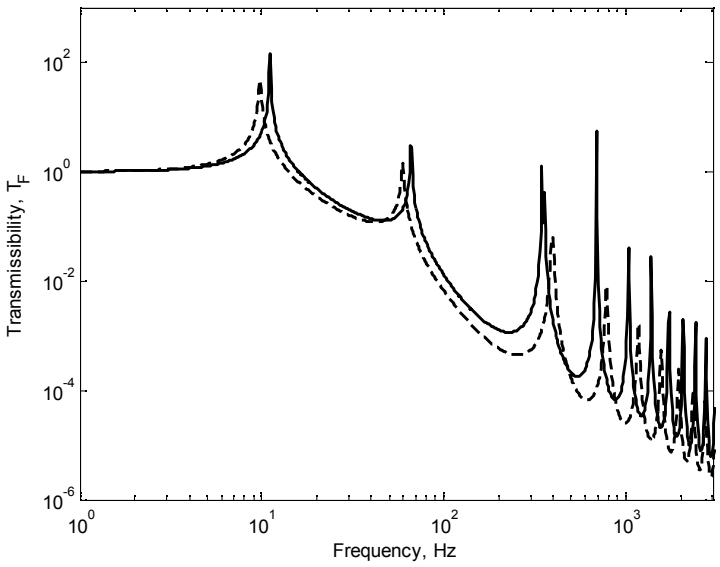

Figure 20. Result for dividing rubber mass into 41 parts
(---: LR-1MS model and ——: discrete lumped parameter system).

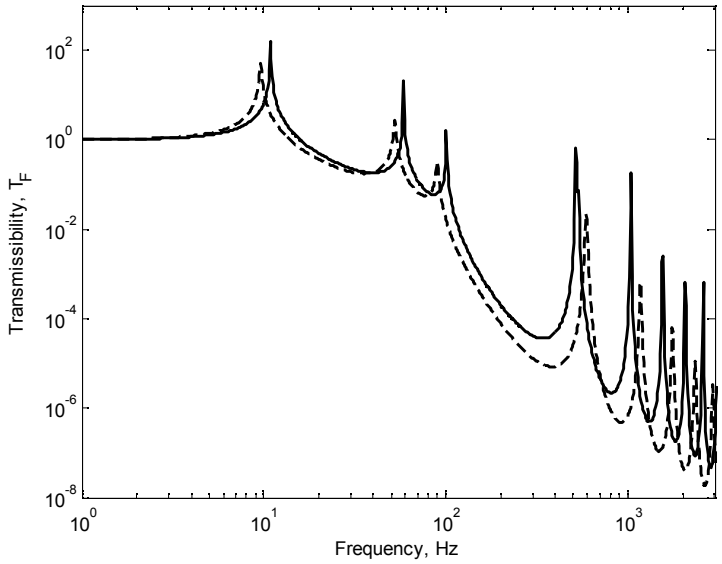

Figure 11. Result for dividing rubber mass into 68 parts
(---: LR-2MS model and ──: discrete lumped parameter system).

4. CONCLUSION

In this paper, it was discussed the mathematical modelling of passive discrete lumped parameter system using Standard Malaysian Rubber Constant Viscosity. It means, the passive vibration isolation performance has been investigated by using basic lumped parameter and then modified it into discrete lumped parameter system. In conventional lumped parameter system, the vibration isolator basically was presumed to be a massless isolator. Then, in high frequencies, the relation showed that the system gives accurate results regarding the isolator performance. The discrete lumped parameter system model was introduced at higher frequencies. Then, by comparing the previous isolator performance, and it shown better. Besides, the trend also similar to conventional model.

In addition, there are two techniques have been used which are lumped parameter system and wave propagation. The lumped parameters system basically focused on the baseline model of the vibration isolator which called as LR-MS in this study. Then, the wave propagation model has been developed using non-dispersive rod and it was elaborated well in this paper. The mathematical modelling which is a prediction tool hope it can have helped to predict the new methodology using trial-error method in future for developing new compounding of vibration isolator.

ACKNOWLEDGEMENTS

Special thanks to the Advanced Academia-Industry Collaboration Laboratory (AiCL) and Fakulti Kejuruteraan Mekanikal (FKM), Universiti Teknikal Malaysia Melaka (UTeM) for providing the laboratory facilities.

REFERENCES

[1] Harrison, M., Sykes, A.O., Martin, M., "*Wave effects in isolation mounts*", Journal of the Acoustical Society of America, **24**, (1952) pp.62-71.

[2] Ruzicka, J. E., & Derby, T. F., "*Influence of damping in vibration isolation*", Shock and Vibration Information Center, (1971).

[4] Idesman, A. V., & Mates, S. P., "*Accurate finite element simulation and experimental study of elastic wave propagation in a long cylinder under impact loading*", International Journal of Impact Engineering, **71**, (2014) pp.1-16.

[3] Pai, P. F., & Nayfeh, A. H., "*Non-linear non-planar oscillations of a cantilever beam under lateral base excitations*", International Journal of Non-Linear Mechanics, **25**(5), (1990) pp.455-474.

[5] Salim, M. A., Abdullah, M. A., & Putra, A., "*Predicted transmissibility of an experimental approach for a laminated rubber-metal spring",* American-Eurasian Journal of Sustainable Agriculture, (2014) pp.104-111.

[6] Salim, M. A., Putra, A., Thompson, D., Ahmad, N., & Abdullah, M. A., "*Transmissibility of a laminated rubber-metal spring: A preliminary study*", In Applied Mechanics and Materials, **393**, (2013) pp.661-665.

[7] Salim, M. A., Saad, A. M., Rosszainily, I. R. A., Wasbari, F., Masripan, N. A., Yusof, N. M., & Al-Mola, M. H. A., "*Evaluation of Mechanical Properties on Vulcanized SMRCV-60 and ENR-25 of Flexible-Rigid Body Vibration Isolator*", International Journal of Nanoelectronics & Materials, **13**, (2020).

[8] Yan, B., Ma, H., Zhang, L., Zheng, W., Wang, K., & Wu, C., "*A bistable vibration isolator with nonlinear electromagnetic shunt damping*", Mechanical Systems and Signal Processing, **136**, (2020) pp.106504.

[9] Bouna, H. S., Nbendjo, B. N., & Woafo, P., "*Isolation performance of a quasi-zero stiffness isolator in vibration isolation of a multi-span continuous beam bridge under pier base vibrating excitation*", Nonlinear Dynamics, **100**(2), (2020) pp.1125-1141.

[10] Ye, K., Ji, J. C., & Brown, T., "*A novel integrated quasi-zero stiffness vibration isolator for coupled translational and rotational vibrations*", Mechanical Systems and Signal Processing, **149**, (2021) pp.107340.

[11] Zhou, X., Sun, X., Zhao, D., Yang, X., & Tang, K., "*The design and analysis of a novel passive quasi-zero stiffness vibration isolator*", Journal of Vibration Engineering & Technologies, **9**(2), (2021) pp.225-245.